

Giant hybridization effects in $4f$ photoemission spectra of Pr and Nd transition-metal compounds

Yu. Kucherenko,* M. Finken, S. L. Molodtsov, M. Heber, J. Boysen, and C. Laubschat
Institut für Oberflächenphysik und Mikrostrukturphysik, TU Dresden, D-01062 Dresden, Germany

G. Behr

Institut für Festkörper und Werkstofforschung Dresden, Postfach 270016, D-01171 Dresden, Germany

(Received 16 January 2002; published 12 April 2002)

Large hybridization effects are observed in $4f$ resonant photoemission spectra of Pr and Nd transition-metal compounds that lead to energy splittings of several eV varying strongly with the composition of the compounds. The phenomena are described quantitatively in the framework of a single-impurity Anderson model. Large splittings of the $4f$ emission are obtained, if the energy position of the expected $4f$ electron-removal state coincides with maxima of the valence-band density of states. For the $4f^n$ ground states, admixtures of $4f^{n+1}$ states of the order of some percents are obtained.

DOI: 10.1103/PhysRevB.65.165119

PACS number(s): 79.60.Bm, 71.20.Eh

During the last decades, more than thousand papers have appeared addressing hybridization effects in Ce systems that are responsible for many-body phenomena such as Kondo-lattices and heavy-fermion behavior. Hybridization effects may be studied directly by photoemission (PE) where they lead to characteristic splittings of the $4f$ -derived PE signal. In addition to the $4f^0$ electron-removal state at about 2 eV binding energy (BE) expected for a simple photoionization of the $4f^1$ ground state of trivalent Ce, one observes a feature close to the Fermi energy (E_F) that reproduces essentially the $4f^1$ final state and is commonly referred as “Kondo peak.”¹ Satellite structures in the Ce $3d$ core-level spectra point also to the presence of final states corresponding to different $4f^n$ configurations. All these phenomena may be described quantitatively in the framework of a single-impurity Anderson model (SIAM),² where the appearance of additional features in the PE spectra is explained in terms of configurational mixing. From the spectroscopically derived model parameters, a consistent description of the ground-state properties of the systems may be obtained.

$4f$ PE spectra of Pr and Nd metals are characterized by single peaks at 3.3 eV and 4.6 eV BE, respectively.³ The spin-orbit split Pr $4f^1$ final state consists basically of the $j = 5/2$ component, since the $j = 7/2$ component contributes only by about 10% of the intensity. In case of the Nd $4f^2$ final-state multiplet effects are more pronounced but spectroscopically unresolved, and lead to a broadening of the $4f$ PE signal. Unlike the pure metals the $4f$ PE spectra of some Pr and Nd transition-metal (TM) compounds reveal large splittings of several eV that are reminiscent of the respective splittings in Ce compounds.⁴ In contrast to the latter, however, there is no peak appearing directly at E_F . Since, simultaneously to the splittings in the $4f$ PE spectra, satellite structures were also observed in the rare-earth (RE) $3d$ core-level spectra,⁵ an interpretation of the experimental data in analogy to Ce was proposed. Quantitative theoretical analyses in the light of SIAM, however, were never attempted, although particularly TM compounds of these elements are of great technological importance due to their magnetic properties. Instead, hybridization phenomena were mostly ignored, and the electronic properties of these compounds

were usually discussed only in the light of Ruderman-Kittel-Kasuya-Yosida and crystal-field effects applied to pure atomiclike $4f$ configurations.

In the present contribution, we show on the basis of a resonant PE study that hybridization leads to $4f^{n+1}$ admixtures of several percents to the $4f^n$ ground states of Pr and Nd TM compounds. PE data were quantitatively analyzed in the framework of the SIAM approach applied usually for the description of Ce systems.² Main parameters in this approach are the energy of a bare $4f^1$ state denoted as ε_f and the hybridization Δ describing the interaction of the $4f$ state with the valence band (VB) via hopping. Introduction of the on-site Coulomb-repulsion energy U_{ff} allows consideration of further configurations with higher $4f$ occupations; hereby, $2\varepsilon_f + U_{ff}$ and $3\varepsilon_f + 3U_{ff}$ describe the energies of the $4f^2$ and $4f^3$ states, respectively. For Ce systems, typical values of these parameters are $\varepsilon_f \cong -2$ eV, $U_{ff} = 7$ eV and $0 < \Delta < 1.5$ eV leading to energy positions of the bare $4f^2$ and $4f^3$ states of 3 eV and 15 eV, respectively. Since the energy difference between the $4f^1$ ground state and the $4f^3$ configuration is large as compared to Δ , the latter does not contribute significantly to configurational mixing and is usually neglected. The situation changes when going from Ce to Pr, where ε_f becomes lowered due to the increase of the nuclear charge. From the analogy to the handling of Ce $3d$ core-level spectra this lowering may be estimated to be of the order of 10 eV (U_{fc}) resulting in energy values of -12 eV, -17 eV, and -15 eV for the bare $4f^1$, $4f^2$, and $4f^3$ states of Pr, respectively. Now, the $4f^0$ configuration is energetically well separated from the $4f^2$ ground state and may be neglected. Shifting the energy zero to the position of the $4f^1$ state and identifying $(\varepsilon_f + U_{ff}) \rightarrow \varepsilon_f$ with the energy necessary to transform a $4f^1$ into a $4f^2$ configuration, one gets formally a projection of Pr back to the Ce problem. An analogous treatment is possible for the case of Nd systems.

The simplest solution of the SIAM is the one presented by Imer and Wuilloud (IW).⁶ Within this approach, the VB is reduced to a single degenerated state at E_F . Although the IW procedure was successfully used for Ce metal, it is not well suited for the description of RE compounds with late TM's,

since these compounds are characterized by large TM d -derived density-of-states (DOS) that are mostly occupied and in some cases shifted away from E_F . A proper description of these systems may be obtained by the solution of the SIAM problem given by Gunnarsson and Schönhammer (GS) (Ref. 2) or, as it will be done in the following, by a simpler approach,⁷ that consists basically of an extension of the IW procedure to various VB states and represents a reasonable approximation of the GS solution.

In the present work, we report on Ce, Pr, and Nd compounds with the late transition elements Rh, Pd, and Ag. Polycrystalline (RE)Ag, (RE)Pd, and (RE)₅Rh₄ samples (RE = Pr, Nd) were prepared by arc-melting under Ar atmosphere, characterized by x-ray diffraction, and cleaned in vacuum by scraping with a diamond file. PrPd₃ and CePd₃ were grown *in-situ* as epitaxial films (thickness about 100 Å) onto W(110) by thermal deposition of the pure constituents under ultrahigh vacuum conditions and subsequent annealing to 600 K.⁸ Sharp low-energy electron-diffraction patterns indicated the formation of the desired AuCu₃(111) structures. PE experiments were performed at room temperature with hemispherical analyzers (VSW AR-65 and VG CLAM-2) using synchrotron radiation from the SX700-II dipole beam line of BESSY I and the U49/2-PGM1 undulator beam line of BESSY II. The pressure during the experiments was better than 10^{-10} mbar and rose shortly to 10^{-9} mbar during film deposition and annealing. Oxygen contaminations were checked monitoring both the O 1s and O 2p signals and were found to be negligible.

The resonant PE spectra of PrAg, PrPd, and Pr₅Rh₄ are shown in Fig. 1. In order to extract $4f$ contributions the on-resonance spectra have been corrected by subtraction of the respective off-resonance data. Due to the large kinetic energy of the photoelectrons surface emissions contribute by less than 20% to the spectra and are, therefore, negligible. The off-resonance spectra of all three compounds consist basically of symmetric peaks with a width of about 2.5 eV FWHM (full width at half maximum). Their energy position shifts with increasing atomic number of the TM element from 2.5 eV BE in Pr₅Rh₄ to 3.2 eV in PrPd and 5.6 eV in PrAg. These peaks reflect emission from TM $4d$ -derived VB states that undergo strong band narrowing as compared to the respective pure TM metals due to the reduced atomic coordination and increased TM-TM distance in the compounds. Emission from the Pr $4f$ states is totally suppressed by the Fano antiresonance. The situation is completely reversed in the on-resonance data, where the nonresonant TM $4d$ contributions amount to only 5% of the spectral intensity. The PE spectra are now dominated by the resonantly enhanced Pr $4f$ emission and consist of a narrow peak at 3.5 eV BE in PrAg, that becomes asymmetrically broadened and shifts to about 2.5 eV BE in PrPd. In Pr₅Rh₄ the $4f$ emission splits into two peaks at about 1.5 eV and 3.8 eV BE, respectively. Apart from these dominant features, a broad shoulder is seen in all spectra at low BE. This shoulder is pinned at the Fermi energy and reflects contributions from resonantly enhanced Pr $5d$ states⁹ that are also visible as weak structures in the off-resonance spectra. To describe the spectra in the framework of our approach to the SIAM, the VB contributions were

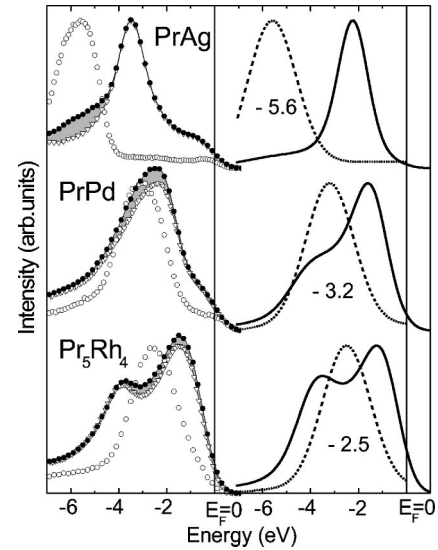


FIG. 1. Left panel: Experimental resonant PE spectra of Pr-TM compounds taken at the Pr $3d \rightarrow 4f$ absorption threshold on-resonance, $h\nu=930$ eV, (●) and off-resonance, $h\nu=923$ eV, (○) with 800 meV overall resolution. Shaded areas represent the nonresonant contributions into the rough on-resonance data. The difference spectra obtained by subtraction of the off-resonance data from the rough on-resonance spectrum are shown by open triangles (▽). The off-resonance and difference spectra are normalized to the equal maximum intensity. Right panel: $4f$ PE spectra (solid lines) calculated for a Gaussian-like DOS (dotted lines; energy positions of Gaussians chosen according to the experimental data and given in the figure). For all spectra model parameters are $\epsilon_f = -2.6$, $\Delta = 1.3$, and $U_{ff} = 7.5$. All energies are in eV.

fitted by Gaussians superimposed by a weak broad semielliptical background. For the calculated spectra (Fig. 1, right panel) the model parameters were chosen in order to describe properly the on-resonance spectrum of Pr₅Rh₄. For didactic reasons (to show the pure effect of changing the energy position of the TM DOS) the same values of the parameters were used to simulate PE spectra of PrPd and PrAg. For Pr₅Rh₄, the energy splitting of the $4f$ emission is due to a quenching of the energy degeneracy of the bare $4f^1$ final state and the narrow DOS. It is analogous to the splitting of interacting valence states into bonding and antibonding orbitals. Good agreement between theory and experiment is achieved, except, that in the experiment the whole $4f$ signal is shifted by about 0.3 eV toward higher BE. Magnitude and direction of this shift correspond to the “impurity term” known from $4f$ PE spectra of heavier RE’s (Ref. 10) that is caused by embedding the final-state ion into the matrix of ground-state atoms. For PrPd and PrAg the model calculations describe the experimental data qualitatively correct. Hybridization effects are strongly reduced due to the increased energy separation between the bare $4f^1$ state and the DOS maximum. Better quantitative agreement between theory and experiment may be obtained for these compounds by decreasing Δ and shifting ϵ_f to higher BE. The first correction takes into account the decreased hybridization due to increasing localization of the TM $4d$ states from Rh to Ag. The second one reflects the so-called chemical shift that de-

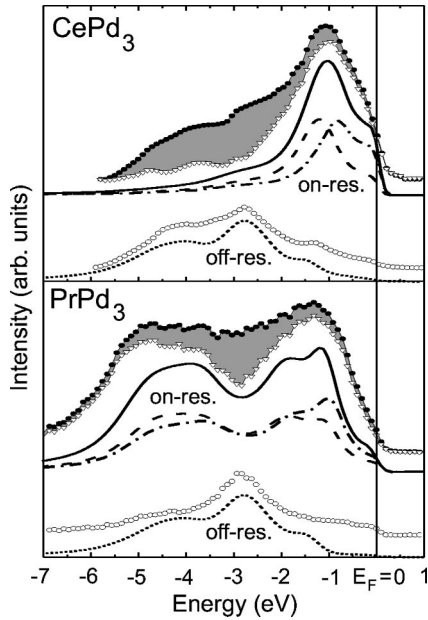


FIG. 2. Experimental on- (●) and off-resonance (○) PE spectra of CePd₃ and PrPd₃ compounds taken at the 4*d*→4*f* absorption threshold with 180 meV overall resolution in comparison with calculated 4*f* emission (solid line) and VB emission (dotted line). Theoretical surface (dashed) and bulk (dash-dotted) contributions to 4*f* emission are also presented. The on-resonance spectra were taken at $h\nu=120$ eV and 130 eV, off-resonance data at $h\nu=112$ eV and 114 eV for the CePd₃ and PrPd₃, respectively. (∇) represent the experimental on-resonance data after correction for nonresonant VB contributions. Experimental data are normalized to the photon flux and corrected by a linear background. The theoretical results are normalized correspondingly to the experimental spectra. Shaded areas as described in the capture to Fig. 1.

scribes mainly the charge transfer between the RE and TM atom.¹⁰ This quantity may be estimated on the basis of thermochemical arguments and leads to shifts toward E_F of increasing magnitude when going from PrAg over PrPd to Pr₅Rh₄.

Instead of shifting the VB position we will tune in the following ϵ_f by comparing isostructural compounds of Pr and Ce. Figure 2 shows resonant PE spectra of CePd₃ and PrPd₃ taken at the 4*d*→4*f* absorption threshold. The shape of the off-resonance spectra is in good agreement with the DOS calculated by means of a linear muffin-tin orbital method.¹¹ For CePd₃ the corrected on-resonance spectrum reveals an asymmetric peak at about 1 eV BE with a pronounced shoulder at E_F , that reflects the well-known splitting of the Ce 4*f* emission into 4*f*⁰ and 4*f*¹ final states. As compared to PE spectra of Ce metal, the energy splitting between these states is remarkably small due to a shift of the 4*f*⁰ component by about 1 eV toward the Fermi energy. For PrPd₃ a double-peaked structure is observed in the on-resonance spectra that extends over more than 5 eV, while the width of the 4*f*¹ final state of Pr metal is smaller than 1 eV. The deep minimum of the corrected resonant 4*f* emission coincides roughly with both the maximum of the DOS and the energy position, where the 4*f*¹ emission of Pr metal is expected.

TABLE I. Parameter values used in the calculations of the PE spectra for CePd₃ and PrPd₃. All energies are in eV.

	Bulk			Surface	
	U_{ff}	ϵ_f	Δ	ϵ_f	Δ
CePd ₃	7.5	-1.25	1.1	-1.60	1.0
PrPd ₃	7.7	-3.00	1.3	-3.35	1.2

In order to describe the 4*f* emission in the framework of SIAM the values of ϵ_f , Δ , and U_{ff} were used as fitting parameters. An additional problem with the analysis of these data stems, however, from the fact that in contrast to the 3*d*→4*f* resonance surface emissions contribute by about 50% of the total intensity at the 4*d*→4*f* absorption threshold and, therefore, should be taken into account. At the surface, ϵ_f is lowered due to the surface core-level shift by about 0.35 eV and Δ is decreased by about 10% due to the reduced coordination in the outermost atomic surface layer.¹² Good agreement between theory and experiment is obtained for parameter values given in Table I. Note that for both compounds Δ is almost the same, and the differences in the intensity distributions are mainly determined by different positions of ϵ_f .

The *f* occupancy is found to be equal to $n_f=0.977$ in the bulk of CePd₃. This value of n_f is very close to that obtained for γ -Ce using almost the same parameter $\epsilon_f=-1.27$ eV.¹³ However, in the bulk PE spectrum of γ -Ce the 4*f*⁰ final-state peak is observed at 1.8 eV BE. Thus, the strong shift of the 4*f*⁰ emission is mainly caused by a “repulsive” character of the interaction with the VB that appears on the high-BE side of ϵ_f in CePd₃ and on the low-BE side of this energy in Ce metal. For PrPd₃ the calculations give a bulk *f* occupancy $n_f=2.025$. In case of PrPd₃ the deviation of n_f from 2 is mainly due to an admixture of about 3% of the 4*f*³ configuration to the ground state, while contributions of the 4*f*¹ configuration are by about a factor of 10 smaller. In case of CePd₃, on the other hand, the 4*f*⁰ and 4*f*² admixtures to the 4*f*¹ ground state amount to 3.4% and 1.1%, respectively.

As an example for a Nd compound, we show finally in Fig. 3 an on-resonance PE spectrum of Nd₅Rh₄. For the

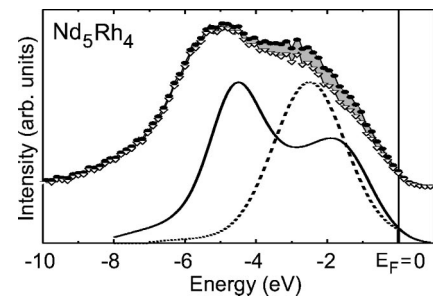


FIG. 3. Experimental on-resonance PE spectrum of Nd₅Rh₄ taken at the 3*d*→4*f* absorption threshold, $h\nu=978.5$ eV, (●) with 800-meV overall resolution and corrected on-resonance data (∇), together with calculated 4*f* emission (solid line) and VB emission (dotted line). Shaded area and normalization as described in the capture to Fig. 1.

model calculations the same Gaussian-like DOS is applied as for Pr_5Rh_4 . The values of parameters are $\varepsilon_f = -3.8$ eV, $\Delta = 1.2$ eV, and $U_{ff} = 7.5$ eV. As in the case of the respective Pr compound the experimental spectrum reveals a splitting of the $4f$ emissions into two components separated from each other by about 2 eV. Again, good qualitative agreement between theory and experiment is achieved, except, that the width of both components is underestimated due to the negligence of multiplet effects. The above-mentioned “impurity term”¹⁰ providing an energy shift of about 0.3 eV toward higher BE is also not taken into account in the calculations. The obtained f occupancy is equal to $n_f = 3.047$ due to almost 5% admixture of the $4f^4$ configuration into the ground state. Note, that in contrast to the respective Pr compound the intensity of the high-BE component is larger than that of the low-BE peak. This is a consequence of the larger absolute value of ε_f that is shifted below the VB maximum. The Δ parameter is slightly decreased as compared to the Pr com-

pound reflecting the increasing localization of the $4f$ states when going from Pr to Nd.

In summary, we have shown that the PE line shapes of the $4f$ emissions in Ce, Pr, and Nd systems are properly described within the framework of SIAM. Large energy splittings of the $4f$ “ionization” peak are obtained, if the position of the expected electron-removal state ε_f coincides with the maximum of the DOS. For ε_f values lying on the low-BE side of the DOS, the maximum of the $4f$ emission is pulled toward E_F , whereas for ε_f values lying on the high-BE side of the DOS the opposite effect is observed. As follows from the calculations, the hybridization in Pr and Nd compounds is of the same order as in Ce systems. For the ground states the hybridization leads in case of Pr and Nd to admixtures of $4f^{n+1}$ configurations by some percents that might have consequences for the magnetic properties of these systems.

This work was supported by the Deutsche Forschungsgemeinschaft, SFB 463, Projects B2, B4, and B11. Expert assistance by the staff of BESSY is acknowledged.

*On leave from Institute of Metal Physics, National Academy of Sciences of Ukraine, UA-03142 Kiev, Ukraine.

¹*Handbook of the Physics and Chemistry of Rare-Earths*, edited by K. A. Gschneidner, L. Eyring, and S. Hüfner (North-Holland, Amsterdam, 1987), Vol. 10.

²O. Gunnarsson and K. Schönhammer, *Phys. Rev. Lett.* **50**, 604 (1983); *Phys. Rev. B* **28**, 4315 (1983); F. Patthey, J.-M. Imer, W.-D. Schneider, H. Beck, and Y. Baer, *ibid.* **42**, 8864 (1990).

³J. K. Lang, Y. Baer, and P. A. Cox, *J. Phys. F: Met. Phys.* **11**, 121 (1981); S. Hüfner, F. Schumann, E. Rotenberg, J. Tobin, S.-H. Yang, B. S. Mun, S. Morton, J. Schfer, and D. Ehm, *Phys. Rev. B* **63**, 085106 (2001).

⁴R. D. Parks, S. Raaen, M. L. den Boer, Y.-S. Chang, and G. P. Williams, *Phys. Rev. Lett.* **52**, 2176 (1984); G. Kalkowski, E. V. Sampathkumaran, C. Laubschat, M. Domke, and G. Kaindl, *Solid State Commun.* **55**, 977 (1985); S. Suga, S. Imada, H. Yamada, Y. Saitoh, T. Nanba, and S. Kunii, *Phys. Rev. B* **52**, 1584 (1995).

⁵F. U. Hillebrecht and J. C. Fuggle, *Phys. Rev. B* **25**, 3550 (1982).

⁶J.-M. Imer and E. Wuilloud, *Z. Phys. B: Condens. Matter* **66**, 153

(1987).

⁷R. Hayn, Yu. Kucherenko, J. J. Hinarejos, S. L. Molodtsov, and C. Laubschat, *Phys. Rev. B* **64**, 115106 (2001).

⁸W. Schneider, S. L. Molodtsov, M. Richter, Th. Gantz, P. Engelmann, and C. Laubschat, *Phys. Rev. B* **57**, 14 930 (1998).

⁹C. G. Olson, P. J. Benning, Michael Schmidt, D. W. Lynch, P. Canfield, and D. M. Wieliczka, *Phys. Rev. Lett.* **76**, 4265 (1996); S. L. Molodtsov, M. Richter, S. Danzenbächer, S. Wieling, L. Steinbeck, and C. Laubschat, *ibid.* **78**, 142 (1997).

¹⁰C. Laubschat, G. Kaindl, W.-D. Schneider, B. Reihl, N. Mårtensson, *Phys. Rev. B* **33**, 6675 (1986).

¹¹O. K. Andersen, *Phys. Rev. B* **12**, 3060 (1975).

¹²C. Laubschat, E. Weschke, C. Holtz, M. Domke, O. Strebler, and G. Kaindl, *Phys. Rev. Lett.* **65**, 1639 (1990); E. Weschke, A. Höhr, G. Kaindl, S. L. Molodtsov, S. Danzenbächer, M. Richter, and C. Laubschat, *Phys. Rev. B* **58**, 3682 (1998); A. Sekiyama, T. Iwasaki, K. Matsuda, Y. Saitoh, Y. Ônuki, and S. Suga, *Nature (London)* **403**, 396 (2000).

¹³L. Z. Liu, J. W. Allen, O. Gunnarsson, N. E. Christensen, and O. K. Andersen, *Phys. Rev. B* **45**, 8934 (1992).